

# Visualization of defects in thin metal plate using scanning airborne ultrasound source technique and dual-frequency guided wave propagation

空中超音波波源走査法と 2 周波ガイド波伝搬を利用した金属薄板内欠陥の可視化

Kyosuke Shimizu<sup>1†</sup>, Ayumu Osumi<sup>2</sup>, and Youichi Ito<sup>2</sup> (<sup>1</sup>Grad. of Sci. & Tech., Nihon Univ.; <sup>2</sup>Coll. of Sci. & Tech., Nihon Univ.)

清水鏡介<sup>1†</sup>, 大隅歩<sup>2</sup>, 伊藤洋一<sup>2</sup> (<sup>1</sup>日大院 理工, <sup>2</sup>日大 理工)

## 1. Introduction

We propose a method that combines an airborne ultrasound phased array (AUPA) with scanning elastic wave source technique<sup>[1]</sup>, which is a non-destructive method for inspecting metal thin plate structures in power plants and chemical plants. To accelerate this method, linear scanning and multi-frequency transmission are combined. In this report, as a basic study, we investigate high-speed non-destructive inspection by scanning elastic wave source technique using two point-focused airborne ultrasound sources with different drive frequencies.

## 2. Measurement principle

Figure 1 is a diagram of the measurement principle, showing the amplitude peak (from Fast Fourier Transform (FFT) analysis) acquired by the receiver when points A and B on the metal thin plate are irradiated with airborne ultrasonic waves to generate guided waves on the thin plate. From Fig. 1, when the thinning area is excited (point A), it bends greatly and gives rise to a large amplitude at the receiver. Therefore, by obtaining the amplitude distribution of the measurement area using scanning measuring, any defects in the thin metal plate can be imaged.

Meanwhile, as shown in Fig. 2 (a), because each measurement point is excited in turn, the measurement time is determined almost entirely by the scanning speed. To shorten the measurement time, it is necessary to perform a linear scan of multiple measurement areas simultaneously as shown in Fig. 2 (b).

In the above measurement, by scanning the sound source with different frequencies, even if guided waves in each measurement region interfere with each other, the peak amplitude for each frequency can be extracted by FFT analysis (Fig. 3).

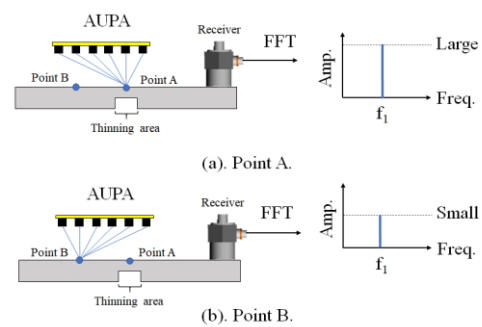


Fig. 1. Measurement principle.

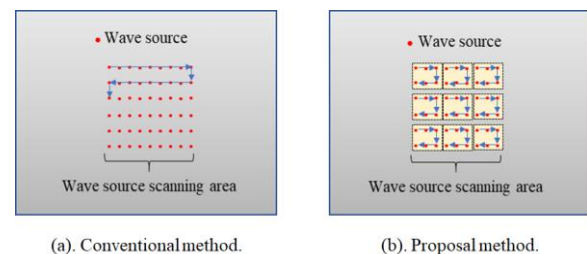


Fig. 2. Wave source scanning method.

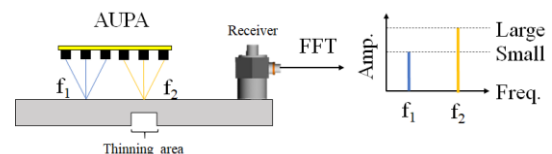


Fig. 3. Measurement principle (proposed version).

## 3. Experimental equipment and method

Figure 4 shows a diagram of the experimental equipment. The device comprises point-focused airborne ultrasound sources, acoustic guides, amplifiers, a function generator, an acoustic emission (AE) sensor, a preamplifier, a data logger, and a personal computer (PC).

Figure 5 shows an outline of the experimental sample. The dimensions of the sample (made of duralumin) were 1000 mm × 300 mm × 3 mm, and a simulated defect of 80 mm × 50 mm was provided at a depth of 0.5 mm from the sample surface.

As shown in Fig. 6, the experimental conditions were that the sample was irradiated with sound waves by scanning a range of 300 mm × 100 mm at 2 mm intervals as excitation area 1 or 2. At this time, guided waves generated in the sample was measured at a fixed point by the AE sensor placed at the red point in the figure. After that, the FFT was performed on the received waveform, and the peak values for each frequency were extracted and stored in an array as shown in Fig. 6.

The sound source was driven at frequencies of 40 and 60 kHz with 10 cycles sine wave, and it was adjusted to have a maximum sound pressure of 1000 Pa. At this time, the two sound sources were arranged so that the distance between the focusing points was 300 mm. The sampling frequency was 2 MHz and the number of samples were 4000.

The experiment was conducted under two different conditions. First, condition 1, excitation area 1 was oscillated at 60 kHz and excitation area 2 was oscillated at 40 kHz; then the experiment was performed condition 2 by exciting excitation area 1 at 40 kHz and excitation area 2 at 60 kHz.

#### 4. Experimental results

The experimental results for condition 1 are shown in Fig. 7, normalized in each measurement range. The results show that in the 60 kHz measurement region, the amplitude increases where the defective part exists, and the latter can be visualized.

Meanwhile, Fig. 8 shows the results for condition 2, again normalized in each measurement range. The results show that in the 40 kHz measurement region, the amplitude increases where the defective part exists, and the latter can be visualized even when the excitation frequency is changed.

#### 5. Conclusion

We reported a basic study of high-speed non-destructive inspection by scanning elastic wave source technique using two point-focused airborne

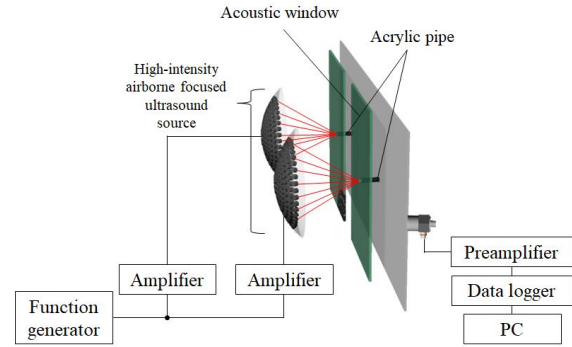


Fig. 4. Experimental equipment.

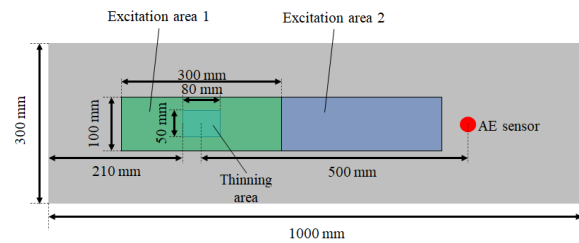


Fig. 5. Sample and measurement area.

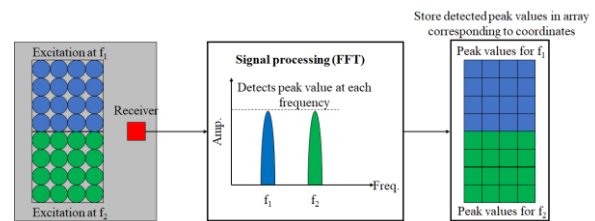


Fig. 6. Overview of processing of experimental data.

ultrasound sources with different drive frequencies. The results confirm that independent visualization results can be obtained and defects can be visualized even when guided waves are generated simultaneously using sound sources of different frequencies.

#### Acknowledgment

This work was partly supported by JSPS KAKENHI Grant number 19K04931.

#### References

1. K. Shimizu, A. Osumi and Y. Ito: Jpn. J. Appl. Phys. 59 (2020) SKKD15.

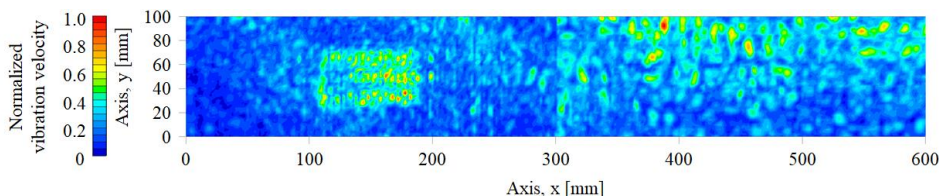


Fig. 7. Experimental results for condition 1.

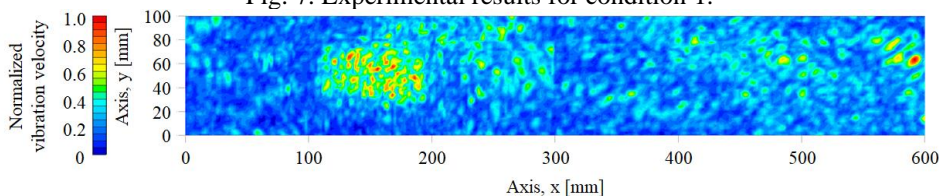


Fig. 8. Experimental results for condition 2.